Journal of
Mechanics of
Materials and Structures

ASYMPTOTIC HOMOGENIZATION MODEL FOR THREE-DIMENSIONAL NETWORK REINFORCED COMPOSITE STRUCTURES

Krishna S. Challagulla, Anastasis Georgiades
and Alexander L. Kalamkarov

Volume 2, Nº 4 April 2007

mathematical sciences publishers

JOURNAL OF MECHANICS OF MATERIALS AND STRUCTURES
Vol. 2, No. 4, 2007

ASYMPTOTIC HOMOGENIZATION MODEL FOR THREE-DIMENSIONAL NETWORK REINFORCED COMPOSITE STRUCTURES

KRISHNA S. CHALLAGULLA, ANASTASIS GEORGIADES AND ALEXANDER L. KALAMKAROV

The method of asymptotic homogenization is used to develop a comprehensive micromechanical model pertaining to three-dimensional composite structures with an embedded periodic network of isotropic reinforcements, the spatial arrangement of which renders the behavior of the given structures macroscopically anisotropic. The model developed in this paper allows the transformation of the original boundary value problem into a simpler one that is characterized by some effective elastic coefficients. These coefficients are calculated from a so-called *unit cell* or periodicity problem, and are shown to depend solely on the geometric and material characteristics of the unit cell and are completely independent of the global formulation of the boundary-value problem. As such, the effective elastic coefficients are universal in nature and can be used to study a wide variety of boundary value problems. The model is illustrated by means of several examples of a practical importance and it is shown that the effective properties of a given composite structure can be tailored to satisfy the requirements of a particular application by changing certain geometric parameters such as the size or relative orientation of the reinforcements. For the special case in which the reinforcements form only a two-dimensional (in-plane) network, the results converge to those of previous models obtained either by means of asymptotic homogenization or by stress-strain relationships in the reinforcements.

1. Introduction

Recent trends have seen the integration of composite materials into new engineering platforms where they replace or strategically compliment other traditional structural materials. Presently, composites can be found in a wide range of applications ranging from sporting and recreational goods, to large-scale structures in the mechanical, aerospace, transportation and civil engineering fields. The continued incorporation of composite materials into new applications can be facilitated if their macroscopic behavior can be predicted at the design stage. To meet this objective, comprehensive micromechanical models must be developed. The effectiveness of such models largely depends on the acknowledgment of the fact that composites have to be approached from two different angles; microscopic and macroscopic. The microscopic view-point addresses the unique behavior and individual characteristics of the various constituents such as the reinforcing fibers and the matrix material, whereas the macroscopic perspective treats the overall composite structure as a single entity. A successful micromechanical model is one which takes both the local and the global aspects of the composite into consideration; it is sophisticated enough to consider the geometrical orientation and mechanical interaction of the various constituents at

Keywords: asymptotic homogenization, composite structures, 3D spatial network, unit cell, effective elastic coefficients.
This work has been supported by the Natural Sciences and Engineering Research Council of Canada (NSERC)..

the local level, but not too convoluted to be readily amenable to analytic and numerical treatments at the macroscopic stress/strain level.

The problem of micromechanical modeling of composites made up of inclusions embedded in a matrix has been the subject of investigation for many years. Among the earlier models developed were the composite spheres model [Hashin 1962] pertinent to macroscopically isotropic composites, and the composite cylinders model proposed by Hashin and Rosen [1964]. In the former model, the inclusions are treated as spherical particles of radius a embedded in a region of matrix of radius b. The absolute size of the particles is allowed to vary, but the ratio of a/b is kept constant. The model was used to estimate the shear and bulk moduli of macroscopically isotropic composites. For the macroscopically anisotropic (in particular, transversely isotropic) composite material, the composite cylinders model treats the reinforcing fibers as cylindrical inclusions of radius a associated with a region of matrix of radius b. As with the composite spheres model, the absolute size of the reinforcements is allowed to vary in order to cover all the available continuous material, but the ratio a/b is kept constant.

Other early work includes the self-consistent scheme [Hill 1965; Budiansky 1965] where a composite is modeled by rigid inclusions embedded in an incompressible matrix, and the Hashin and Shtrikman model [Hashin and Shtrikman 1963a; 1963b]. In their work, Hashin and Shtrikman employed a variational approach to determine upper and lower limits for the effective elastic properties [Hashin and Shtrikman 1963a] as well as electric and thermal conductivities [Hashin and Shtrikman 1963b] of multiphase materials (with quasiisotropic global characteristics). It was discovered that the upper and lower bounds were close to one another (thus representing a reasonably accurate estimate of the properties of the multiphase material) when the properties of the individual constituents were of comparable magnitude. Later on, Milton [1981; 1982] obtained higher-order bounds for the elastic, electromagnetic, and transport properties of two-component composites. Eshelby [1957] studied the case of an ellipsoidal inclusion or inhomogeneity within an infinite matrix and showed that knowing the uniform strain inside the inclusion or homogeneity is sufficient to determine such quantities as the strain fields both near and far from the inclusion/inhomogeneity, the total strain energy in the matrix, etc. Hill [1963] studied the problem of two isotropic media forming perfect bond and having arbitrary volume fractions. Irrespective of the geometry of either component, Hill obtained a complete solution for the special case when these components have equal rigidities but different compressibilities. Russel [1973] studied the problem of slender elastic illusions (of arbitrary cross-section) embedded in a preferred direction within an infinite elastic medium strained uniformly at infinity. His model permitted the calculation of the longitudinal tensile modulus and Poisson's ratio, as well as the bulk modulus of the composite. The author then applied the model to the special case of slender spheroidal inclusions. In the same work, Russel also examined the effect of the inclusion's volume fraction on the elastic properties of the composite. Other work can be found, among others, in [Mori and Tanaka 1973; Sendeckyj 1974; Christensen 1990].

More recently, Drugan and Willis [1996] used the Hashin–Shtrikman variational principle generalized by the second author for random microstructures to derive constitutive equations for two-phase composites of arbitrary isotropy; Kalamkarov and Liu [1998] developed a multiphase fiber-matrix composite material model using a work conjugate approach to derive a so-called mesostructure; Zeman and Šejnoha [2001] used the finite element method to determine effective elastic coefficients of graphite epoxy composites having a random distribution of fibers in a transverse plane section of the composite by extracting an approximate periodicity from the fiber distribution.

Phenomena occurring in composite materials can often be described by means of partial differential equations which are characterized by two vastly different scales: a microscopic scale which reflects the periodicity of the regular composite and a macroscopic scale which is a manifestation of the global formulation of the boundary value problem. The microscopic scale is of the same order of magnitude as the size or spacing of the reinforcements, whereas the macroscopic scale has an order of magnitude similar to a characteristic dimension of the composite structure. The coupling of these two scales in the original problem renders the solution of the pertinent differential equations a very difficult task. To overcome this difficulty, the method of asymptotic homogenization can be used to decouple the microscopic and the macroscopic variations, so that each can be solved independently or sequentially. The mathematical framework of asymptotic homogenization can be found in [Bensoussan et al. 1978; Sanchez-Palencia 1980; Kalamkarov 1992; Cioranescu and Donato 1999; Cioranescu and Paulin 1999] and others. In recent years, asymptotic homogenization methods have been used to analyze periodic composite and smart structures, see, for example, the pioneering work of Duvaut [1976] on inhomogeneous plates; Caillerie [1984] applied a two-scale formalism directly to the three-dimensional problem of a thin nonhomogeneous layer. Accordingly, Caillerie introduced two sets of rapid coordinates. One of these, in the tangential directions, is associated with rapid periodic oscillations in the composite properties. The other is associated with the small thickness of the layer and takes into consideration that there is no periodicity in this transverse direction; Kohn and Vogelius [1984], Kohn and Vogelius [1985] adopted this approach in their study of the pure bending of a thin, linearly elastic homogeneous plate; Guedes and Kikuchi [1990] used a finite element approach to compute effective elastic properties (including error estimates) of composite materials. In his monograph, Kalamkarov [1992], studied a wide variety of elastic and thermoelastic boundary-value problems using the asymptotic homogenization and derived expressions for the effective properties of different structures such as laminated and reinforced plates and shells, infinite cylinders with wavy surfaces, etc; Kalamkarov and Kolpakov [2001] used asymptotic homogenization techniques to derive effective elastic and piezoelectric coefficients for a smart plate; Kalamkarov and Georgiades [2002] applied the asymptotic homogenization method to general 3-dimensional smart composites with nonhomogeneous boundary conditions (which generate boundary-layer like solutions) and obtained effective elastic, piezoelectric, thermal expansion and hygroscopic expansion coefficients. The same authors, Kalamkarov and Georgiades [2004] and Georgiades and Kalamkarov [2004], obtained effective elastic, piezoelectric and thermal expansion coefficients pertinent to wafer- and rib-reinforced smart plates; Georgiades et al. [2006] obtained effective coefficients for thin smart network-reinforced plates.

The present paper develops a novel asymptotic homogenization model for three-dimensional network reinforced composite structures; see Figure 1. In this model, the composite structure is made of periodically arranged unit cells and different elements of unit cell can be made of different materials.

The rest of the paper is organized as follows. The basic problem formulation and model development is presented in Section 2. Section 3 derives the general model for three-dimensional network reinforced composite structures and Section 4 uses it to analyze and discuss various examples. Finally Section 5 concludes the paper.

2. Homogenization model for three-dimensional structures

2.1. ***General model.*** Consider a general composite structure representing an inhomogeneous solid occupying domain G with boundary ∂G that contains a large number of periodically arranged reinforcements as shown in Figure 2.

The elastic deformation of this structure can be described by means of the following set of equations:

$$\frac{\partial \sigma_{ij}^{\varepsilon}}{\partial x_j} = f_i \quad \text{in } G, \qquad \boldsymbol{u}^{\boldsymbol{\varepsilon}}(\boldsymbol{x}) = 0 \quad \text{on } \partial G, \tag{1}$$

where,

$$\sigma_{ij}^{\varepsilon}\left(\boldsymbol{x}, \frac{\boldsymbol{x}}{\varepsilon}\right) = C_{ijkl}\left(\frac{\boldsymbol{x}}{\varepsilon}\right) e_{kl}^{\varepsilon}\left(\boldsymbol{x}, \frac{\boldsymbol{x}}{\varepsilon}\right) \tag{2}$$

$$e_{ij}^{\varepsilon}\left(\boldsymbol{x}, \frac{\boldsymbol{x}}{\varepsilon}\right) = \tfrac{1}{2}\left[\frac{\partial u_i}{\partial x_j}\left(\boldsymbol{x}, \frac{\boldsymbol{x}}{\varepsilon}\right) + \frac{\partial u_j}{\partial x_i}\left(\boldsymbol{x}, \frac{\boldsymbol{x}}{\varepsilon}\right)\right]. \tag{3}$$

Here, C_{ijkl} is the tensor of elastic coefficients, e_{kl} is the strain tensor and $\boldsymbol{u}$ is the displacement field. Finally, f_i represent body forces. The elastic coefficients satisfy the familiar symmetry relationships $C_{ijkl} = C_{jikl} = C_{klij}$ and we assume that they also satisfy the strong convexity relation $C_{ijkl}\chi_{ij}\chi_{kl} > 0$ for any 3×3 real matrix χ_{ij}. It is also assumed in Equation (2) that the C_{ijkl} coefficients are all periodic with a unit cell Y of characteristic dimension ε. It is assumed that ε is made nondimensional by dividing length of unit cell by a certain characteristic dimension of the overall structure. Furthermore, it is assumed that the other two dimensions of the unit cell are of the same order of magnitude as the length. Consequently, the periodic composite structure in Figure 2 is seen to be made up of a large number of unit-cells periodically arranged within the domain G. Let us also note at this point that if the boundary conditions in Equation (1) were made nonhomogeneous, then the resulting field expansions (displacement, strain, etc) would be characterized by boundary-layer type solutions [Kalamkarov and Georgiades 2002]. However, the effective coefficients would not be affected in any way. Thus, for simplicity, homogeneous displacement boundary conditions are chosen here.

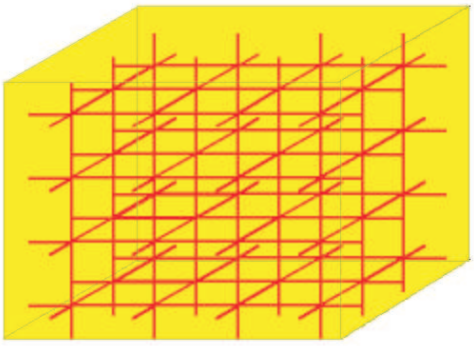

Figure 1. Three-dimensional network reinforced composite structure.

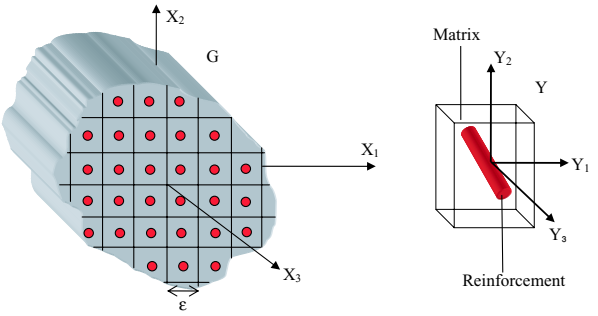

Figure 2. Three-dimensional composite structure with its periodicity (unit) cell.

2.2. ***Asymptotic expansion, governing equation, and unit cell problem.*** Kalamkarov and Georgiades [2002] develops the asymptotic homogenization model for the three-dimensional smart composite structures. In this section, only a brief overview of the steps involved in the development of the model are given in so far as it represents the starting point of our current work. The first step is to define the so-called fast or microscopic variables, as well as new rules of differentiation according to

$$y_i = \frac{x_i}{\varepsilon}, \qquad \frac{\partial}{\partial x_i} \;\rightarrow\; \frac{\partial}{\partial x_i} + \frac{1}{\varepsilon}\frac{\partial}{\partial y_i}. \tag{4}$$

The introduction of these variables transforms the boundary value problem, by separating variables x_i and y_i, and corresponding stress field in Equations (1) and (2) into

$$\frac{\partial \sigma_{ij}^{\varepsilon}}{\partial x_j} + \frac{1}{\varepsilon}\frac{\partial \sigma_{ij}^{\varepsilon}}{\partial y_j} = f_i \quad \text{in } G, \qquad u^{\varepsilon} = 0 \quad \text{on } \partial G, \tag{5}$$

$$\sigma_{ij}^{\varepsilon}(\boldsymbol{x}, \boldsymbol{y}) = C_{ijkl}(\boldsymbol{y})\frac{\partial u_k}{\partial x_l}(\boldsymbol{x}, \boldsymbol{y}). \tag{6}$$

The displacement and stress fields are subsequently expressed as infinite power series in terms of the small parameter ε:

$$\begin{aligned} \boldsymbol{u}^{\varepsilon}(\boldsymbol{x}, \boldsymbol{y}) &= \boldsymbol{u}^{(0)}(\boldsymbol{x}, \boldsymbol{y}) + \varepsilon \boldsymbol{u}^{(1)}(\boldsymbol{x}, \boldsymbol{y}) + \varepsilon^2 \boldsymbol{u}^{(2)}(\boldsymbol{x}, \boldsymbol{y}) + \cdots, \\ \sigma_{ij}^{\varepsilon}(\boldsymbol{x}, \boldsymbol{y}) &= \sigma_{ij}^{(0)}(\boldsymbol{x}, \boldsymbol{y}) + \varepsilon \sigma_{ij}^{(1)}(\boldsymbol{x}, \boldsymbol{y}) + \varepsilon^2 \sigma_{ij}^{(2)}(\boldsymbol{x}, \boldsymbol{y}) + \cdots. \end{aligned} \tag{7}$$

Here all functions in $\boldsymbol{y}$ are periodic with the unit cell Y (see Figure 2). By substituting Equations (4) and (6) into Equation (5) while considering at the same time the periodicity of $\boldsymbol{u}^{(i)}$ in y_j one can readily show that $\boldsymbol{u}^{(0)}$ is independent of the microscopic variable $\boldsymbol{y}$. Subsequently, by substituting Equation (7) into Equation (5) and equating like powers of ε one obtains a sequence of differential equations the first

two of which are

$$\frac{\partial \sigma_{ij}^{(0)}}{\partial y_j} = 0, \tag{8}$$

$$\frac{\partial \sigma_{ij}^{(1)}}{\partial y_j} + \frac{\partial \sigma_{ij}^{(0)}}{\partial x_j} = f_i, \tag{9}$$

where,

$$\sigma_{ij}^{(0)} = C_{ijkl}\left(\frac{\partial u_k^{(0)}}{\partial x_l} + \frac{\partial u_k^{(1)}}{\partial y_l}\right), \tag{10}$$

$$\sigma_{ij}^{(1)} = C_{ijkl}\left(\frac{\partial u_k^{(1)}}{\partial x_l} + \frac{\partial u_k^{(2)}}{\partial y_l}\right). \tag{11}$$

Combination of Equations (8) and (10) yields the following expression:

$$\frac{\partial}{\partial y_j}\left(C_{ijkl}\frac{\partial u_k^{(1)}(\boldsymbol{x}, \boldsymbol{y})}{\partial y_l}\right) = -\frac{\partial C_{ijkl}(\boldsymbol{y})}{\partial y_j}\frac{\partial u_k^{(0)}(\boldsymbol{x})}{\partial x_l}. \tag{12}$$

The separation of variables on the right-hand-side of Equation (12) allows to write down the solution as

$$u_n^{(1)}(\boldsymbol{x}, \boldsymbol{y}) = V_n(\boldsymbol{x}) + \frac{\partial u_k^{(0)}(\boldsymbol{x})}{\partial x_l} N_n^{kl}(\boldsymbol{y}), \tag{13}$$

where functions N_m^{kl} are periodic in $\boldsymbol{y}$ and satisfy

$$\frac{\partial}{\partial y_j}\left(C_{ijmn}(\boldsymbol{y})\frac{\partial N_m^{kl}(\boldsymbol{y})}{\partial y_n}\right) = -\frac{\partial C_{ijkl}}{\partial y_j}. \tag{14}$$

It is seen that Equation (14) depends entirely on the fast variable $\boldsymbol{y}$ and is thus solved on the domain Y of the unit cell remembering at the same time the periodicity of C_{ijkl}, N_m^{kl} in y_i. Consequently, Equation (14) is appropriately referred to as the *unit-cell problem*.

The next important step in the model development is the homogenization process. This is achieved by first substituting Equation (13) into Equation (10) and combining the result with Equation (9). The resulting expression is finally integrated over the domain Y of the unit cell (with volume $|Y|$) remembering to treat x_i as a parameter as far as integration with respect to $\boldsymbol{y}$ is concerned. This gives

$$\frac{1}{|Y|}\int_Y \frac{\partial \sigma_{ij}^{(1)}(\boldsymbol{x}, \boldsymbol{y})}{\partial y_j}\, dv + \tilde{C}_{ijkl}\frac{\partial^2 u_k^{(0)}(\boldsymbol{x})}{\partial x_j \partial x_l} = f_i,$$

where we have defined $\tilde{C}_{ijkl}$ as the effective or homogenized elastic coefficients

$$\tilde{C}_{ijkl} = \frac{1}{|Y|}\int_Y \left(C_{ijkl}(\boldsymbol{y}) + C_{ijmn}(\boldsymbol{y})\frac{\partial N_m^{kl}}{\partial y_n}\right) dv. \tag{15}$$

One observes that the effective coefficients are free from the periodicity complications that characterize their actual rapidly varying material counterparts, C_{ijkl}, and as such, are more amenable to analytical

and numerical treatment. The effective coefficients shown above are universal in nature and can be used to study a wide variety of boundary value problems associated with a given composite structure.

3. Three-dimensional network reinforced composite structures

For the problem at hand, we turn our attention to a general macroscopically anisotropic three-dimensional composite structure reinforced with N families of reinforcements or bars, see, for example, Figure 1, where a particular case of 3 families of reinforcements is shown. The members of each family are made of generally different isotropic materials and are oriented at angles ϕ_1^n, ϕ_2^n, ϕ_3^n, for $n = 1, 2, \ldots, N$, with the y_1, y_2, y_3 axes respectively. Furthermore, they are assumed to be much stiffer than the surrounding matrix so that we are justified in neglecting the contribution of the latter in the ensuing analysis. For the particular case of framework or lattice network structures the surrounding matrix is absent and this is modeled by assuming zero matrix rigidity. The nature of the network structure of Figure 1 is such that it would be more efficient if we first considered a simpler type of unit cell made of only a single reinforcement as shown in Figure 3. Having solved this, the effective elastic coefficients of more general structures with several families of reinforcements can readily be determined by superposition of solution for each of them found separately. In doing so, we accept of course the error incurred at the regions of intersection between the reinforcements, but this error is highly localized and will not add significantly to the integral over the unit cell. A mathematical justification for this kind of argument in the form of the so-called principle of the split homogenized operator has been provided by Bakhvalov and Panasenko [1984]. In order to calculate the effective coefficients for the simpler structure of Figure 3, one must first solve the unit cell problem Equation (14) and then apply the formula in Equation (15).

3.1. ***Problem formulation.*** We begin the problem formulation for the structure of Figure 3 by introducing the following notation:

$$b_{ij}^{kl} = C_{ijmn}(\boldsymbol{y}) \frac{\partial N_m^{kl}(\boldsymbol{y})}{\partial y_n} + C_{ijkl}. \tag{16}$$

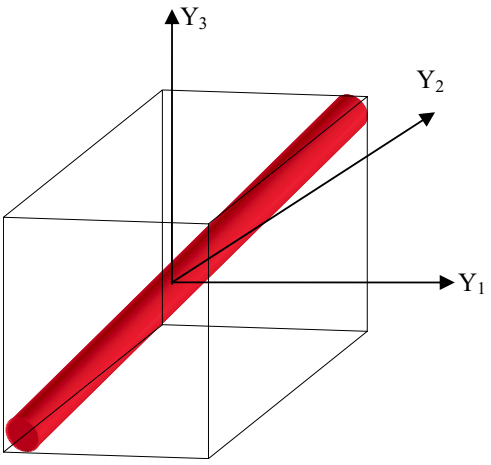

Figure 3. Unit cell of composite network reinforced with a single reinforcement family.

With this definition in mind, the unit cell problem of Equation (14) becomes $\partial\{b_{ij}^{kl}\}/\partial y_j = 0$.

Because of the multiconstituent nature of the network structures under consideration, it is prudent to also consider the interfacial conditions that exist between the matrix and the reinforcements. The first such condition is a direct consequence of the continuity of the $N_m^{kl}(y)$ functions and may be stated as:

$$N_n^{kl}(r)\big|_s = N_n^{kl}(m)\big|_s. \tag{17}$$

Furthermore, continuity of the displacement field leads to:

$$b_{ij}^{kl} n_j(r)\big|_s = b_{ij}^{kl} n_j(m)\big|_s. \tag{18}$$

In Equations (17) and (18) the suffixes s, r, m stand for *interface*, *reinforcement* and *matrix*, respectively. n_j are the components of the unit normal vector to the interface. As mentioned earlier on, we will further assume that the structure of interest is made of high modulus reinforcements and "soft" matrix. As such, we may take $b_{ij}^{kl}(m) \approx 0$ and thus, condition in Equation (18) becomes $b_{ij}^{kl} n_j(r)\big|_s = 0$.

In summary, the final problem that must be solved in conjunction with Equation (17) for the three-dimensional network structure reinforced with a single family of isotropic bars is:

$$\frac{\partial}{\partial y_j}\{b_{ij}^{kl}\} = 0, \qquad b_{ij}^{kl} n_j(r)\big|_s = 0. \tag{19}$$

3.2. ***Coordinate transformation.*** Before proceeding to the solution of the unit cell problem given in Equation (19) we perform a coordinate transformation of the microscopic coordinates $\{y_1, y_2, y_3\}$ onto $\{\eta_1, \eta_2, \eta_3\}$ as shown in Figure 4. The coordinate transformation is carried out in such a way that the η_1 coordinate axis coincides with the direction of the reinforcement and η_2, η_3 are perpendicular to it.

Thus, derivatives transform according to

$$\frac{\partial}{\partial y_i} = q_{ji}\frac{\partial}{\partial \eta_j},$$

where q_{ij} are the components of the matrix of direction cosines characterizing the axis rotation.

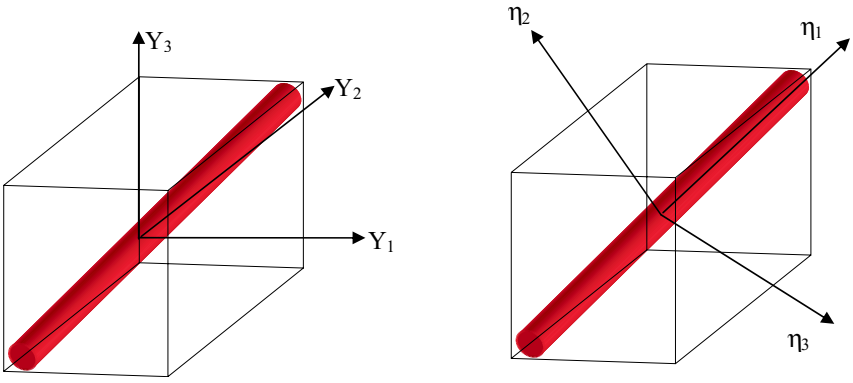

Figure 4. Unit cell in original and rotated macroscopic coordinates.

With this choice of coordinate system, it is evident that problems in Equation (19) will be independent of η_1 and will only depend on η_2 and η_3. Consequently, derivatives with respect to η_1 in the pertinent differential equations vanish and the analysis of the problem is simplified.

3.3. ***Determination of elastic coefficients.*** With reference to Figure 4 we begin by rewriting Equation (19) in terms of the η_i coordinates to get

$$b_{ij}^{kl} = C_{ijmn} q_{pn} \frac{\partial N_m^{kl}}{\partial \eta_p} + C_{ijkl}, \tag{20}$$

$$b_{ij}^{kl} q_{2i} n_2' + b_{ij}^{kl} q_{3i} n_3' \big|_s = 0. \tag{21}$$

Here n_i' represent the components of the unit normal vector expressed in terms of the new coordinates. Expanding Equation (20) remembering at the same time the independence of the problem on η_1 gives:

$$\begin{aligned} b_{ij}^{kl} = C_{ijkl} + C_{ijm1} q_{21} \frac{\partial N_m^{kl}}{\partial \eta_2} + C_{ijm2} q_{22} \frac{\partial N_m^{kl}}{\partial \eta_2} + C_{ijm3} q_{23} \frac{\partial N_m^{kl}}{\partial \eta_2} \\ + C_{ijm1} q_{31} \frac{\partial N_m^{kl}}{\partial \eta_3} + C_{ijm2} q_{32} \frac{\partial N_m^{kl}}{\partial \eta_3} + C_{ijm3} q_{33} \frac{\partial N_m^{kl}}{\partial \eta_3}. \end{aligned} \tag{22}$$

It is possible to solve the system of Equations (20) and (21) by assuming a linear variation of the N_i^{kl} functions in η_2 and η_3, that is,

$$N_1^{kl} = \lambda_1 \eta_2 + \lambda_2 \eta_3, \qquad N_2^{kl} = \lambda_3 \eta_2 + \lambda_4 \eta_3, \qquad N_3^{kl} = \lambda_5 \eta_2 + \lambda_6 \eta_3, \tag{23}$$

where λ_i are constants to be determined from the boundary conditions. It should be noted that the values of the constants λ_i are different for the different combinations of the suffixes k, l in Equation (23) and in the sequel. From Equations (22) and (23), the elastic b_{ij}^{kl} coefficients may be written as follows

$$\begin{aligned} b_{11}^{kl} &= C_{11kl} + C_{11} q_{21} \lambda_1 + C_{11} q_{31} \lambda_2 + C_{12} q_{22} \lambda_3 + C_{12} q_{32} \lambda_4 + C_{13} q_{23} \lambda_5 + C_{13} q_{33} \lambda_6, \\ b_{22}^{kl} &= C_{22kl} + C_{12} q_{21} \lambda_1 + C_{12} q_{31} \lambda_2 + C_{22} q_{22} \lambda_3 + C_{22} q_{32} \lambda_4 + C_{23} q_{23} \lambda_5 + C_{23} q_{33} \lambda_6, \\ b_{33}^{kl} &= C_{33kl} + C_{13} q_{21} \lambda_1 + C_{13} q_{31} \lambda_2 + C_{23} q_{22} \lambda_3 + C_{23} q_{32} \lambda_4 + C_{33} q_{23} \lambda_5 + C_{33} q_{33} \lambda_6, \\ b_{23}^{kl} &= C_{23kl} + C_{44} q_{23} \lambda_3 + C_{44} q_{33} \lambda_4 + C_{44} q_{22} \lambda_5 + C_{44} q_{32} \lambda_6, \\ b_{13}^{kl} &= C_{13kl} + C_{55} q_{23} \lambda_1 + C_{55} q_{33} \lambda_2 + C_{55} q_{21} \lambda_5 + C_{55} q_{31} \lambda_6, \\ b_{12}^{kl} &= C_{12kl} + C_{66} q_{22} \lambda_1 + C_{66} q_{32} \lambda_2 + C_{66} q_{21} \lambda_3 + C_{66} q_{31} \lambda_4. \end{aligned} \tag{24}$$

Here C_{ij} are the elastic coefficients of the isotropic reinforcements in the contracted notation (see, for example, [Reddy 1997]). Substituting Equation (24) in Equation (21) and letting j take on the values 1,

2, 3 results in 6 linear algebraic equations in λ_i for $i = 1, 2, \ldots, 6$

$$\begin{aligned}
A_1\lambda_1 + A_2\lambda_2 + A_3\lambda_3 + A_4\lambda_4 + A_5\lambda_5 + A_6\lambda_6 + A_7 &= 0,\\
A_8\lambda_1 + A_9\lambda_2 + A_{10}\lambda_3 + A_{11}\lambda_4 + A_{12}\lambda_5 + A_{13}\lambda_6 + A_{14} &= 0,\\
A_{15}\lambda_1 + A_{16}\lambda_2 + A_{17}\lambda_3 + A_{18}\lambda_4 + A_{19}\lambda_5 + A_{20}\lambda_6 + A_{21} &= 0,\\
A_{22}\lambda_1 + A_{23}\lambda_2 + A_{24}\lambda_3 + A_{25}\lambda_4 + A_{26}\lambda_5 + A_{27}\lambda_6 + A_{28} &= 0,\\
A_{29}\lambda_1 + A_{30}\lambda_2 + A_{31}\lambda_3 + A_{32}\lambda_4 + A_{33}\lambda_5 + A_{34}\lambda_6 + A_{35} &= 0,\\
A_{36}\lambda_1 + A_{37}\lambda_2 + A_{38}\lambda_3 + A_{39}\lambda_4 + A_{40}\lambda_5 + A_{41}\lambda_6 + A_{42} &= 0,
\end{aligned} \tag{25}$$

where A_i are constants which depend on the direction of the reinforcement as well as its mechanical properties. The explicit expressions for these constants are given in Appendix A. Once the system of Equation (25) is solved, the determined λ_i coefficients are substituted back into Equation (24) to solve for the b_{ij}^{kl} coefficients. In turn, these are used to calculate the effective elastic coefficients of the structure of Figure 3 by integrating over the volume of the unit cell as explained below in Section 3.4. Before closing this section, it would not be amiss to mention that if Equation (23) were assumed to be polynomials of a higher order, then after following the procedure outlined here and comparing terms of equal powers of η_2 and n_3, all of the terms would vanish except the linear ones.

3.4. ***Effective elastic coefficients.*** The effective elastic coefficients of the network composite structure of Figure 3 are obtained by means of the rule of homogenization in Equation (15), which, on account of notation in Equation (16) becomes

$$\tilde{C}_{ijkl} = \frac{1}{|Y|}\int_Y b_{ij}^{kl}\, dv.$$

Assuming that the length (within unit cell), cross-sectional area of the reinforcement and volume of the unit cell in coordinates y_1, y_2, y_3 are L, A, V, respectively, then the effective elastic coefficients are,

$$\tilde{C}_{ijkl} = \frac{AL}{V} b_{ij}^{kl} = V_f b_{ij}^{kl},$$

where b_{ij}^{kl} is constant and V_f is the volume fraction of the reinforcement within the unit cell. It can be proved that the effective elastic coefficients $\tilde{C}_{ijkl}$ satisfy the same symmetry and convexity relationships as their actual material counterparts C_{ijkl} [Bakhvalov and Panasenko 1984].

For network structures with more than a single family of reinforcements, the effective coefficients can be determined by superposition ignoring stress concentration and other local complications at the regions of intersections. For example, for a network composite structure with N families of isotropic reinforcements, the effective elastic coefficients will be given by

$$\tilde{C}_{ijkl} = \sum_{n=1}^{N} V_f^{(n)} b_{ij}^{(n)kl}, \tag{26}$$

where the superscript (n) represents the n-th reinforcement family.

4. Examples of network structures

Let us now apply above developed general theory to the analysis of some examples of practical importance.

Example 1 (Convergence of model for the case of 2D composite network). For the purposes of the first example, we will verify the validity of our model for the case of 2D network structures whereby the reinforcements lie entirely in the Y_2-Y_3 plane. Figure 5 shows the pertinent unit cell for such a structure.

Solving Equation (25) for λ_i and substituting the results into Equation (24) gives the following expressions for the all nonzero elastic coefficients:

$$b_{11}^{11} = E\cos^4\theta, \qquad b_{11}^{12} = E\cos^3\theta\sin\theta, \qquad b_{11}^{22} = b_{12}^{12} = E\cos^2\theta\sin^2\theta,$$
$$b_{22}^{12} = E\cos\theta\sin^3\theta, \qquad b_{22}^{22} = E\sin^4\theta, \qquad b_{ij}^{kl} = b_{kl}^{ij},$$

while the effective coefficients of the composite structure are

$$\tilde{C}_{11} = \frac{AL}{V}E\cos^4\theta, \qquad \tilde{C}_{22} = \frac{AL}{V}E\sin^4\theta, \qquad \tilde{C}_{12} = \tilde{C}_{66} = \frac{AL}{V}E\cos^2\theta\ \sin^2\theta,$$
$$\tilde{C}_{16} = \frac{AL}{V}E\cos^3\theta\ \sin\theta, \qquad \tilde{C}_{26} = \frac{AL}{V}E\cos\theta\sin^3\theta, \qquad \tilde{C}_{ij} = \tilde{C}_{ji}.$$

where we have denoted by E Young's modulus of the reinforcing material. These results are the same as those earlier obtained by Kalamkarov [1992] who developed an asymptotic homogenization model for a thin network-reinforced composite shell and Pshenichnov [1982] who used a different approach based on stress-strain relationships in the reinforcements.

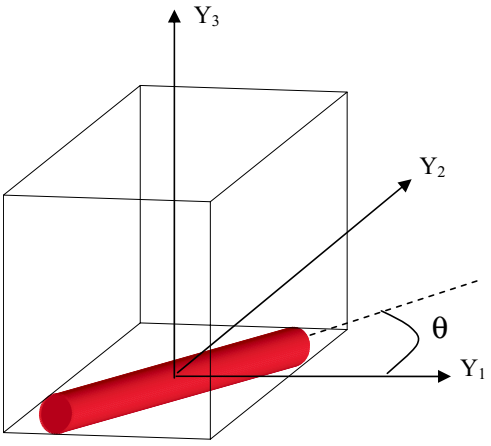

Figure 5. Unit cell for (2D) structure with reinforcements in the Y_1-Y_2 plane.

Example 2. The second example pertains to the cubic structure of Figure 6. This composite structure has three families of reinforcements, each family oriented along one of the coordinate axes.

Noting that $q_{ij} = \delta_{ij}$, where δ_{ij} is the Kronecker symbol, the values of λ_i for the reinforcement in the Y_1 direction are readily obtained from Equation (25) to be as follows

$$\lambda_1 = \frac{-C_{12kl}}{C_{66}}, \qquad \lambda_2 = \frac{-C_{13kl}}{C_{55}}, \qquad \lambda_3 = \frac{C_{33}C_{22kl} - C_{23}C_{33kl}}{{C_{23}}^2 - C_{22}C_{33}},$$
$$\lambda_4 + \lambda_5 = \frac{-C_{23kl}}{C_{44}}, \qquad \lambda_6 = \frac{C_{22}C_{33kl} - C_{23}C_{22kl}}{{C_{23}}^2 - C_{22}C_{33}}.$$

It is observed here that because the transformation tensor q equals the second-order identity sensor, the number of equations is reduced from 6 to 5 and the unknowns λ_4 and λ_5 occur everywhere as the linear combination of $\lambda_4 + \lambda_5$. The same result will occur with reinforcements oriented entirely along either the Y_2 or the Y_3 directions. In both of these cases, a pair of the unknown λ_i occurs as a linear combination and the number of equations is reduced to 5 (with correspondingly 5 unknowns). From Equation (24) the b_{ij}^{kl} coefficients are given by

$$b_{11}^{kl} = C_{11kl} + \frac{[C_{12}C_{33} - C_{13}C_{23}]C_{22kl} + [C_{13}C_{22} - C_{12}C_{23}]C_{33kl}}{C_{23}^2 - C_{22}C_{33}}.$$

After substituting expressions for elastic coefficients we obtain

$$b_{11}^{11} = E, \qquad b_{11}^{22} = b_{11}^{33} = b_{11}^{23} = b_{11}^{13} = b_{11}^{12} = 0, \qquad b_{22}^{kl} = b_{33}^{kl} = b_{23}^{kl} = b_{13}^{kl} = b_{12}^{kl} = 0. \tag{27}$$

Repeating the procedure for the reinforcement in the Y_2 direction yields $b_{22}^{22} = E$ with the remaining coefficients equal to zero, and for the reinforcement in the Y_3 direction the only nonzero coefficient is $b_{33}^{33} = E$.

We are now ready to compute the effective elastic coefficients of the cubic network structures shown in Figure 6. Let the length (within unit cell) and cross-sectional area of the i-th reinforcement in the Y_i direction be L_i and A_i respectively (in coordinates y_1, y_2, y_3). Also let us assume that E_i is the Young's modulus of the reinforcement in the Y_i direction. Then, for a unit cell of volume V, the corresponding volume fraction v_i is given by $v_i = A_i L_i / V$. Thus, from Equations (26) and (27) the nonzero effective elastic coefficients for the composite network structure of Figure 6 are

$$\tilde{C}_{11} = \frac{A_1 L_1}{V} E_{(1)} = v_1 E_{(1)}, \qquad \tilde{C}_{22} = \frac{A_2 L_2}{V} E_{(2)} = v_2 E_{(2)}, \qquad \tilde{C}_{33} = \frac{A_3 L_3}{V} E_{(3)} = v_3 E_{(3)}, \tag{28}$$

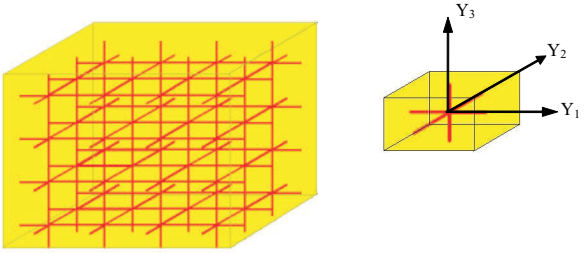

Figure 6. Cubic network structure with reinforcements in Y_1, Y_2, Y_3 directions.

where $E_{(i)}$ is the young's modulus of the i-th reinforcement. In the case where the reinforcements have the same material properties (namely Young's modulus E) the expressions in Equation (28) become

$$\tilde{C}_{11} = \frac{A_1}{V}E = v_1 E, \qquad \tilde{C}_{22} = \frac{A_2}{V}E = v_2 E, \qquad \tilde{C}_{33} = \frac{A_3}{V}E = v_3 E.$$

It is observed that all the off-diagonal terms in the stiffness matrix are zero. This is partly because the reinforcements in a particular direction have no effect on the stiffness of the structure in the directions perpendicular to it and partly due to the fact that the matrix stiffness is neglected in this model.

Example 3. This example pertains to a composite network structure with a conical arrangement of isotropic reinforcements. In this example (to be referred to as structure S_1) the unit cell is made of three reinforcements oriented as shown in Figure 7. The expressions for the effective coefficients are readily determined from Equations (24)–(26). Although the expressions are too lengthy to be reproduced here, some of these coefficients will be presented graphically in the next section.

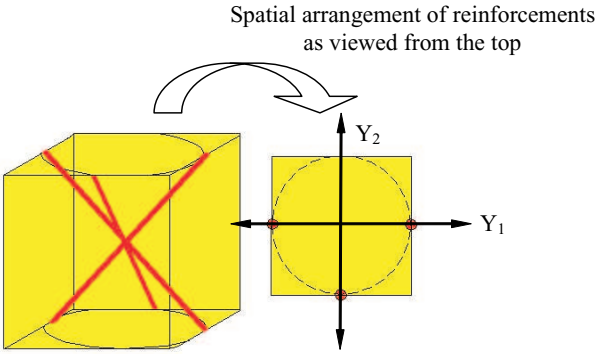

Figure 7. Unit cell for composite network structure with conical arrangement of isotropic reinforcements (structure S_1).

Example 4. In this example let us consider a general unit cell (S_2) as shown in Figure 8. The general unit cell consists of three reinforcements two of which span from different corners of the unit cell to the diametrically opposite ones and the third reinforcement is oriented from the middle of the bottom edge to the middle of the top edge on the opposite face.

The effective coefficients for this structure are calculated as for the ones in the previous examples. The resulting expressions are too lengthy to be reproduced here. However as an illustration some of the effective coefficients are plotted vs. the height of the unit-cell in the following section.

4.1. ***Plots of effective properties and discussion.*** The mathematical model and methodology presented in Sections 3.1–3.4 can be used in analysis and design to tailor the effective elastic coefficients of any three-dimensional composite network structure by changing the material, number, orientation and/or cross-sectional area and material selection of the reinforcements. In this section typical effective coefficients will be computed and plotted. For illustration purposes, we will assume that the reinforcements have a Young's modulus and Poisson's ratio equal to 200 GPa and 0.3, respectively.

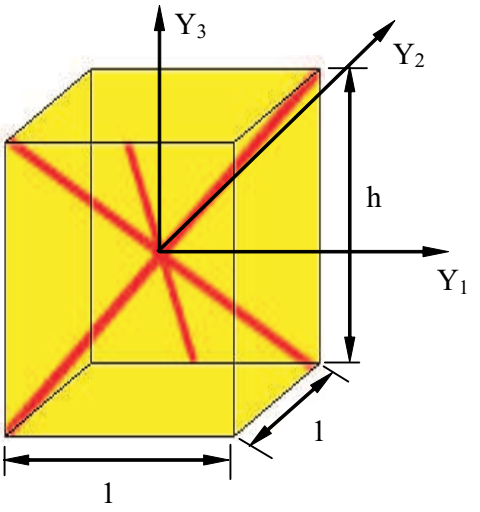

Figure 8. Structure S_2.

We will begin with the plot of some of the effective coefficients for the structure shown in Figure 7. The effective coefficients will be plotted vs. the total volume fraction of the reinforcements within the unit cell. As expected, the effective coefficients increase with an increase in the overall reinforcement volume fraction, see for example Figures 9 and 10.

It would also be of interest to plot the variation of some of the effective coefficients of structure S_1 with the angle of inclination of the reinforcements to the Y_3 axis. As this angle increases, the reinforcements are oriented progressively closer to the Y_1 and Y_2 axis and the stiffness in these directions is expected to increase. Indeed a reference to Figures 11 and 12 shows precisely that. On the contrary, (see Figure 13) at the same time as the stiffness in the Y_1 and Y_2 directions increases the corresponding value in the Y_3 direction decreases because the reinforcements are oriented further away from the Y_3 axis.

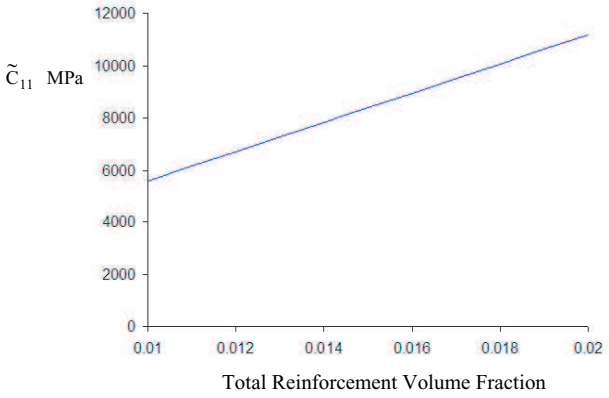

Figure 9. Plot of $\tilde{C}_{11}$ vs. reinforcement volume fraction for structure S_1.

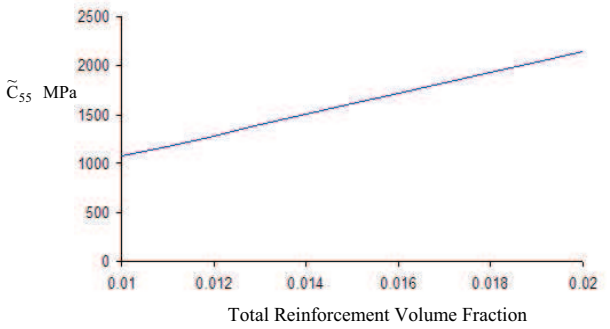

Figure 10. Plot of $\tilde{C}_{55}$ vs. reinforcement volume fraction for structure S_1.

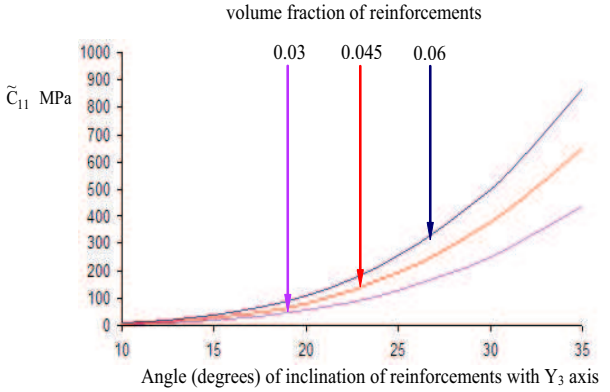

Figure 11. Plot of the $\tilde{C}_{11}$ effective coefficient vs. inclination of reinforcements with the Y_3 axis pertaining to structure S_1 for reinforcement volume fractions equal to 0.03, 0.045, and 0.06.

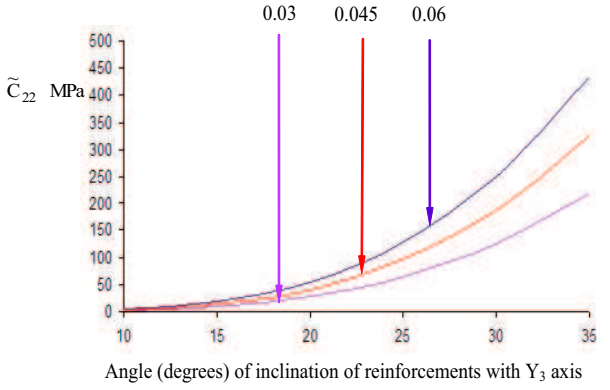

Figure 12. Plot of the $\tilde{C}_{22}$ effective coefficient vs. inclination of reinforcements with the Y_3 axis pertaining to structure S_1 for reinforcement volume fractions equal to 0.03, 0.045, and 0.06.

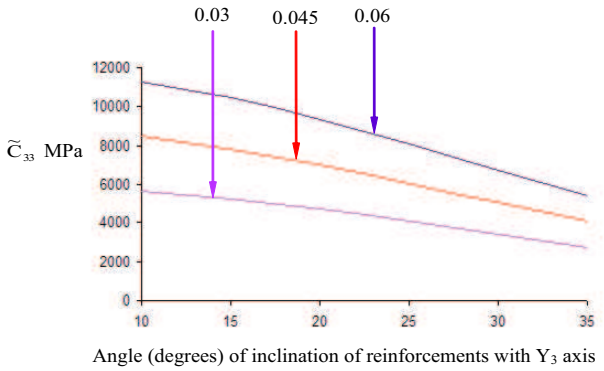

Figure 13. Plot of the $\tilde{C}_{33}$ effective coefficient vs. inclination of reinforcements with the Y_3 axis pertaining to structure S_1 for reinforcement volume fractions equal to 0.03, 0.045, and 0.06.

We now turn our attention to the S_2 composite structure (Figure 8) and plot some of the effective coefficients by varying the relative height of the unit cell (height divided by length) but keeping the other dimensions as well as the cross-sectional area of the reinforcements constant. It is noted that as the relative height of the unit cell is varied, the lengths and orientations of reinforcements change.

Figure 14 shows a plot of effective coefficients $\tilde{C}_{11}$, $\tilde{C}_{22}$, $\tilde{C}_{33}$, and $\tilde{C}_{55}$ vs. the relative height of the unit cell. As the relative height of the unit-cell increases, the volume fraction of the reinforcements decreases and at the same time the reinforcements are oriented closer to the Y_3 axis and further away from Y_1, and Y_2 axis. Both of these effects contribute to the stiffness in the Y_1, and Y_2 direction decreasing. However, $\tilde{C}_{33}$ increases because the increase in stiffness due to a smaller angle of inclination with the Y_3 axis dominates the decrease in stiffness due to the reinforcements volume fraction decreasing.

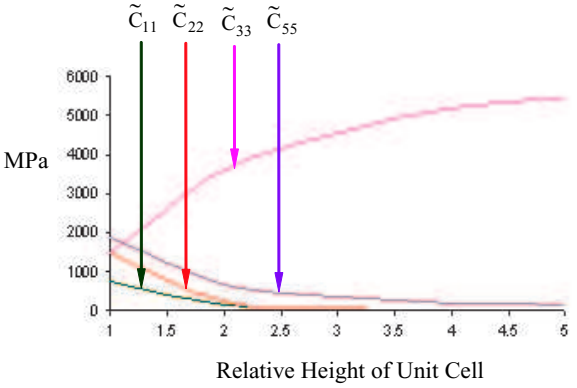

Figure 14. Plot of $\tilde{C}_{11}$, $\tilde{C}_{22}$, $\tilde{C}_{33}$, and $\tilde{C}_{55}$ effective coefficient vs. relative height of the unit cell for S_2 structure shown in Figure 8.

Finally, we are interested to compare a typical effective coefficient of structures S_1 and S_2 by varying the volume fraction. We vary the volume fraction of structure S_1 by varying the reinforcement cross-sectional area and of structure S_2 by varying the relative height of the unit cell. From Figure 15 we see that $\tilde{C}_{33}$ for S_1 increases as the volume fraction increases, as expected for larger diameter reinforcements. However, pertinent to structure S_2, increasing the volume fraction of the reinforcements is tantamount to decreasing the relative height of the unit cell. This has the effect of increasing the deviation of the reinforcements from the Y_3 axis which dominates the increase in the overall reinforcement volume fraction. Consequently, the net effect is that a decrease in the relative height of the unit cell produces a reduction (in a nonlinear fashion) in the stiffness of the composite structure in the Y_3 direction. Thus, under these circumstances, beyond a certain volume fraction, S_1 is stiffer in the Y_3 direction. Of course these trends can be easily changed. For example, if the volume fraction of the reinforcements of S_2 is changed by keeping all dimensions of unit cell constant (that is, direction cosines pertinent to reinforcements unchanged) and changing their cross-sectional area, then a higher volume fraction would increase $\tilde{C}_{33}$, and the relative stiffness between the two structures would be different than that depicted in Figure 15. What is important is to realize that the model allows for complete flexibility in designing a structure with desirable mechanical and geometrical characteristics.

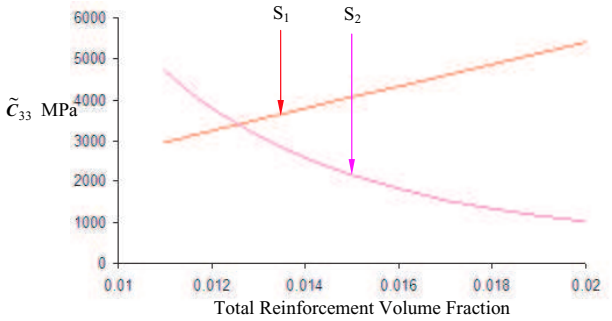

Figure 15. Plot of $\tilde{C}_{33}$ vs. total volume fraction for structures S_1 (Figure 7) and S_2 (Figure 8).

5. Conclusions

A comprehensive three-dimensional micromechanical model pertaining to globally anisotropic periodic composite structures reinforced with a spatial network of isotropic reinforcements is developed. The model, which is developed using the asymptotic homogenization technique, transforms the original boundary value problem into a simpler one that is characterized by some effective elastic coefficients. The effective coefficients are shown to depend only on the pertinent geometric and material characteristics of the periodicity cell and are therefore independent of the global formulation of the problem.

The derived model is illustrated by means of different composite structures with cubic or conical configurations of reinforcements. The usefulness of this work lies in the fact that the model can be used to tailor the effective coefficients of any three-dimensional composite structure to meet the requirements of a particular application by changing such geometric or other parameters as the material, number,

cross-sectional dimensions, and relative angular orientation of the reinforcements. In the particular case in which the reinforcements form only a two-dimensional (planar) network, the results are shown to converge to previous models developed by Kalamkarov [1992] who also used the asymptotic homogenization technique and Pshenichnov [1982] who used stress-strain relationships in the reinforcements.

Appendix A

$$
\begin{aligned}
A_1 &= {q_{21}}^2 C_{11} + {q_{22}}^2 C_{66} + {q_{23}}^2 C_{55}, & A_2 &= q_{21}q_{31}C_{11} + q_{22}q_{32}C_{66} + q_{23}q_{33}C_{55},\\
A_3 &= q_{21}q_{22}C_{12} + q_{21}q_{22}C_{66}, & A_4 &= q_{21}q_{32}C_{12} + q_{22}q_{31}C_{66},\\
A_5 &= q_{21}q_{23}C_{13} + q_{21}q_{23}C_{55}, & A_6 &= q_{21}q_{33}C_{13} + q_{23}q_{31}C_{55},\\
A_7 &= q_{21}C_{11kl} + q_{22}C_{12kl} + q_{23}C_{13kl}, & A_8 &= q_{21}q_{31}C_{11} + q_{22}q_{32}C_{66} + q_{23}q_{33}C_{55},\\
A_9 &= {q_{31}}^2 C_{11} + {q_{32}}^2 C_{66} + {q_{33}}^2 C_{55}, & A_{10} &= q_{31}q_{22}C_{12} + q_{21}q_{32}C_{66},\\
A_{11} &= q_{31}q_{32}C_{12} + q_{32}q_{31}C_{66}, & A_{12} &= q_{31}q_{23}C_{13} + q_{21}q_{33}C_{55},\\
A_{13} &= q_{31}q_{33}C_{13} + q_{33}q_{31}C_{55}, & A_{14} &= q_{31}C_{11kl} + q_{32}C_{12kl} + q_{33}C_{13kl},\\
A_{15} &= q_{21}q_{22}C_{66} + q_{21}q_{22}C_{12}, & A_{16} &= q_{21}q_{32}C_{66} + q_{22}q_{31}C_{12},\\
A_{17} &= {q_{21}}^2 C_{66} + {q_{22}}^2 C_{22} + {q_{23}}^2 C_{44}, & A_{18} &= q_{21}q_{31}C_{66} + q_{22}q_{32}C_{22} + q_{23}q_{33}C_{44},\\
A_{19} &= q_{22}q_{23}C_{23} + q_{22}q_{23}C_{44}, & A_{20} &= q_{22}q_{33}C_{23} + q_{23}q_{32}C_{44},\\
A_{21} &= q_{21}C_{12kl} + q_{22}C_{22kl} + q_{23}C_{23kl}, & A_{22} &= q_{31}q_{22}C_{66} + q_{21}q_{32}C_{12},\\
A_{23} &= q_{31}q_{32}C_{66} + q_{32}q_{31}C_{12}, & A_{24} &= q_{21}q_{31}C_{66} + q_{22}q_{32}C_{22} + q_{23}q_{33}C_{44},\\
A_{25} &= {q_{31}}^2 C_{66} + {q_{32}}^2 C_{22} + {q_{33}}^2 C_{44}, & A_{26} &= q_{32}q_{23}C_{23} + q_{22}q_{33}C_{44},\\
A_{27} &= q_{32}q_{33}C_{23} + q_{33}q_{32}C_{44}, & A_{28} &= q_{31}C_{12kl} + q_{32}C_{22kl} + q_{33}C_{23kl},\\
A_{29} &= q_{21}q_{23}C_{55} + q_{21}q_{23}C_{13}, & A_{30} &= q_{21}q_{33}C_{55} + q_{23}q_{31}C_{13},\\
A_{31} &= q_{22}q_{23}C_{44} + q_{22}q_{23}C_{23}, & A_{32} &= q_{22}q_{33}C_{44} + q_{23}q_{32}C_{23},\\
A_{33} &= {q_{21}}^2 C_{55} + {q_{22}}^2 C_{44} + {q_{23}}^2 C_{33}, & A_{34} &= q_{21}q_{31}C_{55} + q_{22}q_{32}C_{44} + q_{23}q_{33}C_{33},\\
A_{35} &= q_{21}C_{13kl} + q_{22}C_{23kl} + q_{23}C_{33kl}, & A_{36} &= q_{31}q_{23}C_{55} + q_{21}q_{33}C_{13},\\
A_{37} &= q_{31}q_{33}C_{55} + q_{33}q_{31}C_{13}, & A_{38} &= q_{23}q_{32}C_{44} + q_{22}q_{33}C_{23},\\
A_{39} &= q_{32}q_{33}C_{44} + q_{33}q_{32}C_{23}, & A_{40} &= q_{21}q_{31}C_{55} + q_{22}q_{32}C_{44} + q_{23}q_{33}C_{33},\\
A_{41} &= {q_{31}}^2 C_{55} + {q_{32}}^2 C_{44} + {q_{33}}^2 C_{33}, & A_{42} &= q_{31}C_{13kl} + q_{32}C_{23kl} + q_{33}C_{33kl}.
\end{aligned}
$$

References

[Bakhvalov and Panasenko 1984] N. Bakhvalov and G. Panasenko, *Homogenisation: averaging processes in periodic media*, Kluwer Academic Publishers, Netherlands, 1984.

[Bensoussan et al. 1978] A. Bensoussan, J. L. Lions, and G. Papanicolaou, *Asymptotic analysis for periodic structures*, North-Holland Publ. Comp., Amsterdam, 1978.

[Budiansky 1965] B. Budiansky, "On the elastic moduli of some heterogeneous materials", *J. Mech. Phys. Solids* **13** (1965), 223–227.

[Caillerie 1984] D. Caillerie, "Thin elastic and periodic plates", *Math. Appl. Sci.* **6** (1984), 159–191.

[Christensen 1990] R. M. Christensen, "A critical evaluation for a class for a class of micromechanics models", *J. Mech. Phys. Solids* **38** (1990), 379–404.

[Cioranescu and Donato 1999] D. Cioranescu and P. Donato, *An introduction to homogenization*, Oxford University Press, Oxford, United Kingdom, 1999.

[Cioranescu and Paulin 1999] D. Cioranescu and J. S. J. Paulin, *Homogenization of reticulated structures*, Springer-Verlag, New York, 1999.

[Drugan and Willis 1996] W. J. Drugan and J. R. Willis, "A micromechanics-based nonlocal constitutive equation and estimates of representative volume element size for elastic composites", *J. Mech. Phys. Solids* **44**:4 (1996), 497–524.

[Duvaut 1976] G. Duvaut, "Analyse fonctionnelle et mécanique des milieux continues", pp. 119–132 in *Proceedings of the 14^{th} IUTAM congress*, Delft, 1976.

[Eshelby 1957] J. D. Eshelby, "The determination of the elastic field of an ellipsoidal inclusion, and related problems", *Proc. R. Soc. Lond.* **A241** (1957), 376–396.

[Georgiades and Kalamkarov 2004] A. V. Georgiades and A. L. Kalamkarov, "Asymptotic homogenization models for smart composite plates with rapidly varying thickness: part II-applications", *Int. J. Multiscale Computational Engineering* **2**:1 (2004), 149–172.

[Georgiades et al. 2006] A. V. Georgiades, A. L. Kalamkarov, and K. S. Challagulla, "Asymptotic homogenization model for smart network composite reinforced plates", *Smart Mater. Struct.* **15** (2006), 1197–1210.

[Guedes and Kikuchi 1990] J. M. Guedes and N. Kikuchi, "Preprocessing and postprocessing for materials based on the homogenization method with adaptive finite element methods", *Comput. Methods Appl. Mech. Eng.* **83** (1990), 143–198.

[Hashin 1962] Z. Hashin, "The elastic moduli of heterogeneous materials", *J. Appl. Mech.* **29** (1962), 143.

[Hashin and Rosen 1964] Z. Hashin and B. W. Rosen, "The elastic moduli of fiber-reinforced materials", *J. Appl. Mech.* **31** (1964), 223–232.

[Hashin and Shtrikman 1963a] Z. Hashin and S. Shtrikman, "A variational approach to the theory of elastic behavior of multiphase materials", *J. Mech. Phys. Solids* **11** (1963a), 127–140.

[Hashin and Shtrikman 1963b] Z. Hashin and S. Shtrikman, "Conductivity of polycrystals", *Phys. Rev.* **130**:1 (1963b), 129–133.

[Hill 1963] R. Hill, "Elastic properties of reinforced solids", *J. Mech. Phys. Solids* **11** (1963), 357–372.

[Hill 1965] R. Hill, "A self-consistent mechanics of composite materials", *J. Mech. Phys. Solids* **13** (1965), 213–222.

[Kalamkarov 1992] A. L. Kalamkarov, *Composite and reinforced elements of construction*, Wiley, Chichester, UK, 1992.

[Kalamkarov and Georgiades 2002] A. L. Kalamkarov and A. V. Georgiades, "Micromechanical modeling of smart composite structures", *Smart Mater. Struct.* **11** (2002), 423–434.

[Kalamkarov and Georgiades 2004] A. L. Kalamkarov and A. V. Georgiades, "Asymptotic homogenization models for smart composite plates with rapidly varying thickness: part I-theory", *Int. J. Multiscale Computational Engineering* **2**:1 (2004), 133–148.

[Kalamkarov and Kolpakov 2001] A. L. Kalamkarov and A. G. Kolpakov, "A new asymptotic model for a composite piezoelastic plate", *Int. J. Solids Struct.* **38** (2001), 6027–6044.

[Kalamkarov and Liu 1998] A. L. Kalamkarov and H. Q. Liu, "A new model for a multiphase fiber-matrix composite materials", *Compos. B: Eng.* **29B**:5 (1998), 643–653.

[Kohn and Vogelius 1984] R. V. Kohn and M. Vogelius, "A new model for thin plates with rapidly varying thickness", *Int. J. Solids Struct.* **20** (1984), 333–350.

[Kohn and Vogelius 1985] R. V. Kohn and M. Vogelius, "A new model for thin plates with rapidly varying thickness, II: a convergence proof", *Quart. J. Appl. Math.* **43** (1985), 1–22.

[Milton 1981] G. W. Milton, "Bounds on the electromagnetic, elastic, and other properties of two-component composites", *Phys. Rev. Lett.* **46** (1981), 542–545.

[Milton 1982] G. W. Milton, "Bounds on the elastic and transport properties of two-component composites", *J. Mech. Phys. Solids* **30** (1982), 177–191.

[Mori and Tanaka 1973] T. Mori and K. Tanaka, "Average stress in matrix and average energy of materials with misfitting inclusions", *Acta. Metall. Mater.* **21** (1973), 571–574.

[Pshenichnov 1982] G. I. Pshenichnov, *Theory of thin elastic network plates and shells*, Nauka, Moscow, 1982. In Russian.

[Reddy 1997] J. N. Reddy, *Mechanics of laminated composite plates*, CRC Press, New York, 1997.

[Russel 1973] W. B. Russel, "On the effective moduli of composite materials: effect of fiber length and geometry at dilute concentrations", *Z. Angew. Math. Phys.* **24** (1973), 581–600.

[Sanchez-Palencia 1980] E. Sanchez-Palencia, *Non-homogeneous media and vibration theory*, Springer-Verlag, Berlin, 1980.

[Sendeckyj 1974] G. P. Sendeckyj, *Elastic behavior of composites*, Composite Materials, Vol. 2. Mechanics of composite materials, Academic Press, New York, 1974.

[Zeman and Šejnoha 2001] J. Zeman and M. Šejnoha, "Numerical evaluation of effective elastic properties of graphite fiber tow impregnated by polymer matrix", *J. Mech. Phys. Solids* **49** (2001), 69–90.

Received 21 Jun 2006. Accepted 1 Oct 2006.

KRISHNA S. CHALLAGULLA: kchallag@dal.ca
Department of Mechanical Engineering, Dalhousie University, Halifax, Nova Scotia, B3J 2X4, Canada

ANASTASIS GEORGIADES: tasos.georgiades@dal.ca
Department of Mechanical Engineering, Dalhousie University, Halifax, Nova Scotia, B3J 2X4, Canada

ALEXANDER L. KALAMKAROV: alex.kalamkarov@dal.ca
Department of Mechanical Engineering, Dalhousie University, Halifax, Nova Scotia, B3J 2X4, Canada